John von Neumann Institute for Computing

Hadron Masses and Nucleon Matrix Elements

Gerrit Schierholz

published in

NIC Symposium 2006 ,
G. Münster, D. Wolf, M. Kremer (Editors),
John von Neumann Institute for Computing, Jülich,
NIC Series, Vol. **32**, ISBN 3-00-017351-X, pp. 109-116, 2006.

http://www.fz-juelich.de/nic-series/volume32

Hadron Masses and Nucleon Matrix Elements

Gerrit Schierholz

NIC, DESY Zeuthen
Platanenallee 6, 15738 Zeuthen, Germany
E-mail: gsch@mail.desy.de

We[1] present first results from a simulation of quenched overlap fermions with improved gauge field action. Among the quantities we study are the hadron masses and selected nucleon matrix elements. To make contact with continuum physics, we compute the renormalization constants of quark bilinear operators nonperturbatively.

1 Introduction

Lattice calculations at small quark masses, i.e. in the chiral regime, require actions with good chiral properties. Overlap fermions[2] have an exact chiral symmetry on the lattice[3] and thus are predestinated for this task. A further advantage of overlap fermions is that they are automatically $O(a)$ improved[4].

Previous calculations of hadron observables from quenched overlap fermions have been limited to larger quark masses and/or coarser lattices due to the high cost of the simulations[5–8]. To ensure that the correlation functions involved are not overshadowed by the exponential decay of the overlap operator[9], the lattice spacing a should be small enough. Ideally $m_H a \ll 1$, where m_H is the mass of the hadron. In addition, the spatial extent of the lattice L should satisfy $L \gg 1/(2f_\pi)$ in order to be able to make contact with chiral perturbation theory[10].

Over the past years we have done extensive simulations of quenched overlap fermions[7,11,12]. In this contribution we shall report a few of our results on hadron masses and nucleon structure functions.

The massive overlap operator is defined by

$$D = \left(1 - \frac{am_q}{2\rho}\right) D_N + m_q \tag{1}$$

with the Neuberger-Dirac operator D_N given by

$$D_N = \frac{\rho}{a}\left(1 + \frac{D_W(\rho)}{\sqrt{D_W^\dagger(\rho) D_W(\rho)}}\right), \quad D_W(\rho) = D_W - \frac{\rho}{a}, \tag{2}$$

where D_W is the massless Wilson-Dirac operator with $r = 1$, and $\rho \in [0, 2]$ is a (negative) mass parameter. The operator D_N has $n_- + n_+$ exact zero modes, $D_N \psi_n^0 = 0$ with $n = 1, \cdots, n_- + n_+$, where n_- (n_+) denotes the number of modes with negative (positive) chirality, $\gamma_5 \psi_n^0 = -\psi_n^0$ ($\gamma_5 \psi_n^0 = +\psi_n^0$). The index of D_N is thus given by $\nu = n_- - n_+$. The 'continuous' modes λ_i, $D_N \psi_i = \lambda_i \psi_i$, satisfy $(\psi_i^\dagger, \gamma_5 \psi_i) = 0$ and come in complex conjugate pairs λ_i, λ_i^*.

To evaluate D_N it is appropriate to introduce the hermitean Wilson-Dirac operator $H_W(\rho) = \gamma_5 D_W(\rho)$, such that

$$D_N = \frac{\rho}{a}\left(1 + \gamma_5 \,\mathrm{sgn}\{H_W(\rho)\}\right), \tag{3}$$

where $\mathrm{sgn}\{H\} = H/\sqrt{H^2}$. The sign function can be defined by means of the spectral decomposition

$$\mathrm{sgn}\{H_W(\rho)\} = \sum_i \mathrm{sgn}\{\mu_i\}\, \chi_i \chi_i^\dagger \,, \tag{4}$$

where χ_i are the normalized eigenvectors of $H_W(\rho)$ with eigenvalue μ_i. Equation (4) is, however, not suitable for numerical evaluation. We write

$$\mathrm{sgn}\{H_W(\rho)\} = \sum_{i=1}^{N} \mathrm{sgn}\{\mu_i\}\, \chi_i \chi_i^\dagger + P_\perp^N H_W(\rho) \,, \tag{5}$$

where

$$P_\perp^N = 1 - \sum_{i=1}^{N} \chi_i \chi_i^\dagger \tag{6}$$

projects onto the subspace orthogonal to the eigenvectors of the N lowest eigenvalues of $|H_W(\rho)|$, and approximate $P_\perp^N H_W(\rho)$ by a minmax polynomial[13]. More precisely, we construct a polynomial $P(x)$, such that

$$\left| P(x) - \frac{1}{\sqrt{x}} \right| < \epsilon \,, \quad x \in [\mu_{N+1}^2, \mu_{\max}^2] \,, \tag{7}$$

where μ_{N+1} ($\mu_{\max}$) is the lowest (largest) eigenvalue of $|P_\perp^N H_W(\rho)|$. We then have

$$\mathrm{sgn}\{H_W(\rho)\} = \sum_{i=1}^{N} \mathrm{sgn}\{\mu_i\}\, \chi_i \chi_i^\dagger + P_\perp^N H_W(\rho)\, P(H_W^2(\rho)) \,. \tag{8}$$

The degree of the polynomial will depend on ϵ and on the condition number of $H_W^2(\rho)$, $\kappa = \mu_{\max}^2/\mu_{N+1}^2$, on the subspace $\{\chi_i \,|\, (1 - P_\perp^N)\chi_i = 0\}$.

We use the Lüscher-Weisz gauge action[14]

$$S[U] = \frac{6}{g^2} \left[c_0 \sum_{\text{plaquette}} \frac{1}{3} \,\mathrm{Re\,Tr}\,(1 - U_{\text{plaquette}}) + c_1 \sum_{\text{rectangle}} \frac{1}{3} \,\mathrm{Re\,Tr}\,(1 - U_{\text{rectangle}}) \right.$$
$$\left. + c_2 \sum_{\text{parallelogram}} \frac{1}{3} \,\mathrm{Re\,Tr}\,(1 - U_{\text{parallelogram}}) \right] \,, \tag{9}$$

where $U_{\text{plaquette}}$ is the standard plaquette, $U_{\text{rectangle}}$ denotes the closed loop along the links of the 1×2 rectangle, and $U_{\text{parallelogram}}$ denotes the closed loop along the diagonally opposite links of the cubes. The coefficients c_1, c_2 are taken from tadpole improved perturbation theory[15]:

$$\frac{c_1}{c_0} = -\frac{(1 + 0.4805\alpha)}{20 u_0^2} \,, \quad \frac{c_2}{c_0} = -\frac{0.03325\alpha}{u_0^2} \tag{10}$$

with $c_0 + 8c_1 + 8c_2 = 1$, where

$$u_0 = \left(\frac{1}{3} \mathrm{Tr}\, \langle U_{\text{plaquette}} \rangle \right)^{\frac{1}{4}} \,, \quad \alpha = -\frac{\log(u_0^4)}{3.06839} \,. \tag{11}$$

β	V	am_q						
8.00	$16^3\,32$	0.0168	0.0280	0.0420	0.0560	0.0840	0.1400	0.1960
8.45	$16^3\,32$				0.0280	0.0560	0.0980	0.1400
8.45	$24^3\,48$		0.0112	0.0196	0.0280	0.0560	0.0980	0.1400

Table 1. Couplings, lattice volumes and mass parameters of the simulation.

We write

$$\beta = \frac{6}{g^2}\, c_0\,. \tag{12}$$

After having fixed β, the parameters c_1, c_2 are determined. In the classical continuum limit $u_0 \to 1$ the coefficients c_1, c_2 assume the tree-level Symanzik values[16] $c_1 = -1/12$, $c_2 = 0$.

The simulations are done on the lattices and at the quark masses listed in Table 1. We set the scale by the scale parameter r_0. In the literature we find[15] $r_0/a = 3.69(4)$ at $\beta = 8.0$ and $r_0/a = 5.29(7)$ at $\beta = 8.45$, respectively. Taking $r_0 = 0.5$ fm, this results in the lattice spacings 0.135 fm at $\beta = 8.0$ and 0.09 fm at $\beta = 8.45$, respectively. The couplings have been chosen such that the $16^3\,32$ lattice at $\beta = 8.0$ and the $24^3\,48$ lattice at $\beta = 8.45$ have approximately the same physical volume. This allows us to study both scaling violations and finite size effects.

We have projected out $N = 40$ lowest lying eigenvectors at $\beta = 8.0$ and $N = 50$ ($N = 10$) at $\beta = 8.45$ on the $24^3\,48$ ($16^3\,32$) lattice. These numbers scale roughly with the physical volume of the lattice. The degree of the polynomial P has been adjusted such that $1/\sqrt{H_W^2(\rho)}$ is determined with a relative accuracy of better than 10^{-7}.

The mass parameter ρ influences the simulation in two ways. First, it affects the locality properties[9] of the Neuberger-Dirac operator. Secondly, the condition number of $P_\perp^N H_W^2(\rho)$, $\kappa = \mu_{\max}^2/\mu_{N+1}^2$, depends on ρ as well. We have chosen $\rho = 1.4$, which is a trade-off between a small condition number κ and good locality properties. Our simulations cover the range of pseudoscalar masses $250 \lesssim m_{PS} \lesssim 900\,\mathrm{MeV}$ as we shall see. The lowest quark mass was chosen such that $m_{PS} L \gtrsim 3$. On all our lattices we have $L \gg 1/(2f_\pi)$.

$O(a)$ improvement, both for masses and on- and off-shell operator matrix elements, is achieved by simply replacing D_N by[4]

$$D_N^{\mathrm{imp}} \equiv \left(1 - \frac{aD_N}{2\rho}\right)^{-1} D_N \tag{13}$$

in the calculation of the quark propagator. In the following we shall always use the improved propagator, without mentioning this explicitly. While the eigenvalues of D_N lie on a circle of radius ρ around $(\rho, 0)$ in the complex plane, the eigenvalues of D_N^{imp} fall onto the imaginary axis.

The inversion of the overlap operator D is done by solving the system of equations

$$Ax = y\,, \tag{14}$$

where $A = D^\dagger D$ and y is a suitable vector. We use the conjugate gradient algorithm for that. The speed of convergence depends on the condition number of the operator A,

$\kappa(A) = \nu_{\max}/\nu_{\min}$, where $\nu_{\max}$ ($\nu_{\min}$) is the largest (lowest) eigenvalue of A. For reasonable values of the quark mass we have $\kappa(A) \propto 1/m_q^2$. Thus, the number of iterations, n_D, needed to achieve a certain accuracy will grow like $n_D \propto 1/m_q$ as the quark mass is decreased.

The convergence of the algorithm can be accelerated by a preconditioning method. Instead of (14) we solve the equivalent system of equations

$$ACx = Cy \equiv \tilde{A}x\,, \tag{15}$$

where C is a nonsingular matrix, which we choose such that $\kappa(\tilde{A}) \ll \kappa(A)$. Our choice is

$$C = 1 + \sum_{i=1}^{n} \left(\frac{1}{\nu_i} - 1 \right) v_i\, v_i^\dagger\,, \tag{16}$$

where v_i (ν_i) are the normalized eigenvectors (eigenvalues) of A. The condition number of the operator $\tilde{A}$ is by a factor ν_{n+1}/ν_1 smaller than the condition number of the operator A, and the number of iterations in the conjugate gradient algorithm reduces to $n_D \propto 1/\sqrt{\nu_{n+1} + m_q^2}$, which depends only weakly on the quark mass m_q. We have chosen $n = 80$, and the inversion was stopped when a relative accuracy of 10^{-7} was reached.

In the calculation of meson and baryon correlation functions we use smeared sources to improve the overlap with the ground state, while the sinks are taken to be either smeared or local. We use Jacobi smearing for source and sink[17]. To set the size of the source, we have chosen $\kappa_s = 0.21$ for the smearing hopping parameter and employed $N_s = 50$ smearing steps.

To further improve the signal of the correlation functions, we have deployed low mode averaging by breaking the quark propagator into two pieces,

$$\sum_{i=1}^{n_\ell} \frac{\psi_i(x)\psi_i^\dagger(y)}{(1 - am_q/2\rho)\,\lambda_i + m_q}\,, \tag{17}$$

where the sum extends over the eigenmodes of the n_ℓ lowest eigenvalues (including the zero modes), and the remainder. The contribution from the low-lying modes (17) is averaged over all positions of the quark sources. As the largest contribution to the correlation functions comes from the lower modes, we may expect a significant improvement in the regime of small quark masses. We have chosen $n_\ell = 40$, mainly because of memory limitations.

2 Hadron Masses

Let us now turn to the calculation of hadron masses. We consider hadrons where all quarks have degenerate masses. So far we have generated $200 - 600$ independent gauge field configurations on each of our lattices.

To compute the pseudoscalar mass, m_{PS}, we looked at correlation functions of the pseudoscalar density $P = \bar{q}\gamma_5 q$ and the time component of the axial vector current $A_4 = \bar{q}\gamma_4\gamma_5 q$. Local sinks are found to give slightly smaller error bars than smeared sinks, so that we will restrict ourselves to this case. Both correlators give consistent results. We will use the results from the axial vector current correlator here.

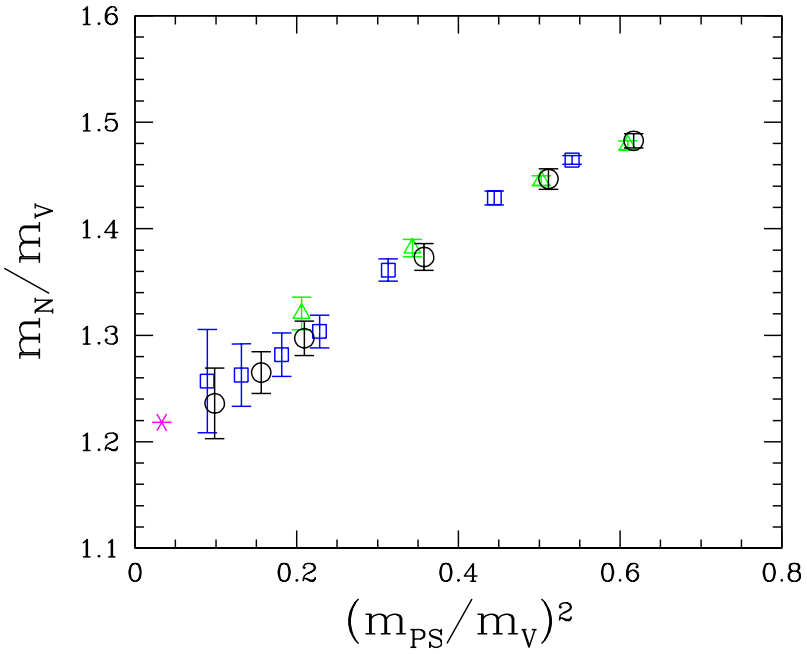

Figure 1. APE plot on the $24^3\,48$ lattice at $\beta = 8.45$ ($\bigcirc$) and on the $16^3\,32$ lattices at $\beta = 8.0$ ($\square$) and $\beta = 8.45$ ($\triangle$), together with the experimental value ($*$).

To compute the vector meson mass, m_V, we explored correlation functions of operators $V_i = \bar{q}\gamma_i q$ and $V_i^4 = \bar{q}\gamma_i\gamma_4 q$ ($i = 1, 2, 3$). We found that the operator V_i, in combination with a local sink, gives the best signal.

For the calculation of the nucleon mass, m_N, we used $B_\mu = \varepsilon_{abc} q_\mu^a (q^b C\gamma_5 q^c)$ (where $C = \gamma_4\gamma_2$) as our basic operator, where we have replaced each spinor by $q \to q^{NR} = (1/2)(1+\gamma_4)q$[17]. These so-called nonrelativistic wave functions have a better overlap with the ground state than the ordinary, relativistic ones. The nucleon mass is obtained from a fit of the data by the correlation function $A\exp(-m_N t) + B\exp(-m_{N^*}(T-t))$ (where T is the time extent of the lattice and m_{N^*} the mass of the backward moving baryon).

In Fig. 1 we show our results in form of an APE plot for our three lattices. At our smallest quark masses we have $m_{PS}/m_V \approx 0.3$, which is the lowest quark mass reached so far in any lattice simulation.

3 Nucleon Matrix Elements

Information about the internal structure of the nucleon is encoded in its structure functions. While they cannot be computed directly on the lattice, the operator product expansion (OPE) provides a connection between their moments and nucleon matrix elements of local operators. For the unpolarized structure function F_1 the OPE reads

$$2\int_0^1 dx x^{n-1} F_1(x, Q^2) = \sum_q E^q_{F_1,n} v^q_n + O(1/Q^2)\,, \tag{18}$$

where q denotes the quark flavour, $E^q_{F_1,n}$ is the (perturbative) Wilson coefficient, and the matrix element v^q_n is defined by

$$\langle N(\vec{p})| \left(O^q_{\{\mu_1 \ldots \mu_n\}} - \text{traces} \right) |N(\vec{p})\rangle = 2 v^q_n (p_{\mu_1} \ldots p_{\mu_n} - \text{traces}) \,, \tag{19}$$

where

$$O^q_{\mu_1 \ldots \mu_n} = \bar{q} \gamma_{\mu_1} \overleftrightarrow{D}_{\mu_2} \ldots \overleftrightarrow{D}_{\mu_n} q \,. \tag{20}$$

Similar relations hold for the other structure functions[17]. Both, the matrix element v^q_n and the Wilson coefficient $E^q_{F_1,n}$ depend upon the choice of a renormalization scheme and scale. Only in their product these dependencies cancel.

To compute the matrix elements (19) we consider the ratio[17]

$$R = \frac{\langle N(t_{sink}) O(\tau) \bar{N}(t_{source}) \rangle}{\langle N(t_{sink}) \bar{N}(t_{source}) \rangle} \,, \tag{21}$$

from which v^q_n can be determined in the region $t_{source} < \tau < t_{sink}$. We always set $t_{source} = 0$ and $t_{sink} = 9$ ($t_{sink} = 13$) in lattice units at $\beta = 8.0$ ($\beta = 8.45$), which corresponds to a distance between source and sink of 1.4 fm.

For lack of space we are only considering the operator

$$O^q_{44} - \tfrac{1}{3} \left(O^q_{11} + O^q_{22} + O^q_{33} \right) \tag{22}$$

and flavor nonsinglet combinations, i.e. u - d (u and d labelling u and d quark, respectively) corresponding to proton minus neutron structure function. In this case there is no contribution from disconnected diagrams.

The operator (22) needs to be renormalized. It is logarithmically divergent. We compute the renormalization factors in the $\mathrm{RI}' - \mathrm{MOM}$ scheme[18]. In this scheme the renormalization condition is formulated in terms of quark Greens functions, computed in Landau gauge, with an operator insertion at zero momentum transfer:

$$C_O(p) = \frac{1}{V} \sum_{x,y,z} e^{-ip(x-y)} \langle q(x) O(z) \bar{q}(y) \rangle \,. \tag{23}$$

From this quantity we compute the amputated vertex function Γ_O,

$$\Gamma_O(p) = S^{-1}(p) C_O(p) S^{-1}(p) \,, \tag{24}$$

where the quark propagator is given by

$$S(p) = \frac{1}{V} \sum_{x,y} e^{-ip(x-y)} \langle q(x) \bar{q}(y) \rangle \,. \tag{25}$$

The renormalization condition at scale μ is

$$Z_q(\mu) Z_O(\mu) \Pi_O \left(\Gamma_O(p) \right)|_{p^2=\mu^2} = 1 \tag{26}$$

with $\Pi_O(\Gamma_O(p)) = \frac{1}{12} \mathrm{tr} \left(\Gamma^{-1}_{O,\mathrm{Born}}(p) \Gamma_O(p) \right)$. The wave function renormalization constant Z_q is determined from the relation $Z_q Z_A \Pi_A \left(\Gamma_A \right) = 1$.

In order to convert the results to the $\overline{\mathrm{MS}}$ scheme, we first determine the renormalization group invariant renormalization constant Z^{RGI}_O,

$$Z^{\mathrm{RGI}}_O = \left(Z^{\mathrm{RI}'-\mathrm{MOM,RGI}}_O(\mu) \right)^{-1} Z^{\mathrm{RI}'-\mathrm{MOM}}_O(\mu) \,, \tag{27}$$

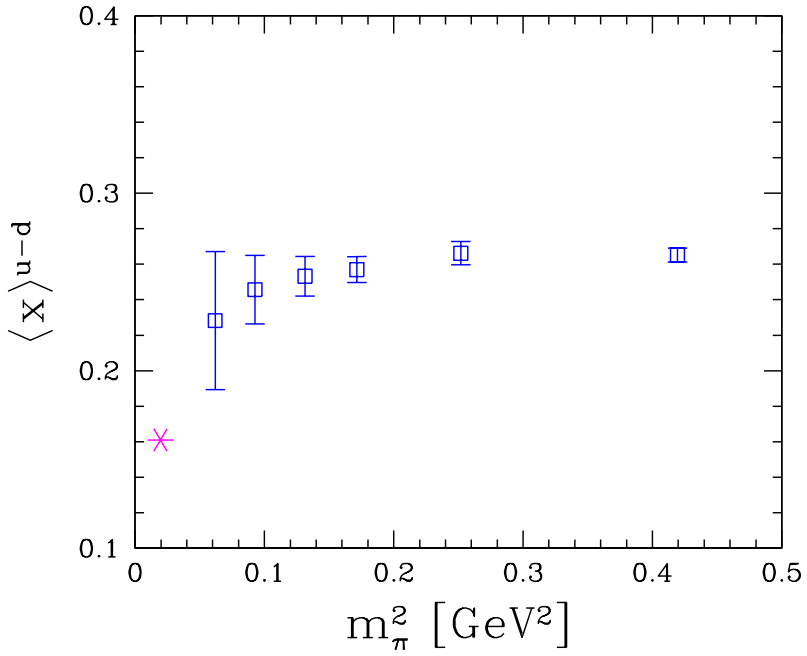

Figure 2. The first moment $\langle x^{u-d} \rangle$ of the unpolarized proton minus neutron structure function on the $16^3\,32$ lattice at $\beta = 8.0$ as a function of the pion mass in the $\overline{\rm MS}$ scheme at 2 GeV, together with the phenomenological value ($*$).

and then convert to the $\overline{\rm MS}$ scheme at scale μ' by $Z_O^{\overline{\rm MS}}(\mu') = Z_O^{\overline{\rm MS},{\rm RGI}}(\mu) Z_O^{\rm RGI}$. The conversion functions to the scheme $\mathcal{S}$ are given by

$$Z_O^{\mathcal{S},{\rm RGI}}(\mu) = \left(2 b_1 g^{\mathcal{S}}(\mu)^2\right)^{-\frac{d_{O,1}}{2b_1}} \exp\left[\int_0^{g^{\mathcal{S}}(\mu)} d\xi \left(\frac{\gamma_O^{\mathcal{S}}(\xi)}{\beta^{\mathcal{S}}(\xi)} + \frac{d_{O,1}}{b_1 \xi}\right)\right]. \qquad (28)$$

The coefficients of the β and γ functions are taken from Ref. 19.

We obtain $Z_{O_{44}}^{\rm RGI} = 2.9$ at $\beta = 8.0$ and $Z_{O_{44}}^{\rm RGI} = 2.6$ at $\beta = 8.45$, respectively. Using $Z_{O_{44}}^{\overline{\rm MS},{\rm RGI}}(2\,{\rm GeV}) = 0.737$, we finally obtain $Z_{O_{44}}^{\overline{\rm MS}} = 2.11$ at $\beta = 8.0$ and $Z_{O_{44}}^{\overline{\rm MS}} = 1.92$ at $\beta = 8.45$, respectively. A comparison with results obtained in one-loop tadpole-improved lattice perturbation theory[20] shows large discrepancies, telling us that the renormalization of lattice operators has to be done nonperturbatively.

Our results for $v_2^{u-d} \equiv \langle x \rangle^{u-d}$ are shown in Fig. 2. We see that the lattice numbers start to bend down towards the phenomenological value, but only at pion masses $\lesssim 350$ MeV. At the larger quark masses our results agree with previous results obtained from improved Wilson fermions[17].

4 Conclusions

It is important to do simulations at small quark masses, in order to reliably extrapolate the lattice results to the chiral limit. Overlap fermions allow us to do so. By the time this article goes to print we will have doubled our statistics. We hope that NIC will grant us the CPU time to perform simulations with dynamical overlap fermions in the near future.

References

1. In collaboration with M. Gürtler, R. Horsley, H. Perlt, P. E. L. Rakow, A. Schiller and T. Streuer.
2. H. Neuberger, Phys. Lett. B417 (1998) 141; *ibid.* B427 (19998) 353.
3. M. Lüscher, Phys. Lett. B428 (1998) 342.
4. S. Capitani, M. Göckeler, R. Horsley, P. E. L. Rakow and G. Schierholz, Phys. Lett. B468 (1999) 150.
5. L. Giusti, C. Hoelbling and C. Rebbi, Phys. Rev. D64 (2001) 114508 [Erratum *ibid.* D65 (2002) 079903]; N. Garron, L. Giusti, C. Hoelbling, L. Lellouch and C. Rebbi, Phys. Rev. Lett. 92 (2004) 042001; F. Berruto, N. Garron, C. Hoelbling, J. Howard, L. Lellouch, S. Necco, C. Rebbi and N. Shoresh, Nucl. Phys. Proc. Suppl. 140 (2005) 264.
6. S. J. Dong, F. X. Lee, K. F. Liu and J. B. Zhang, Phys. Rev. Lett. 85 (2000) 5051; S. J. Dong, T. Draper, I. Horvath, F. X. Lee, K. F. Liu and J. B. Zhang, Phys. Rev. D65 (2002) 054507; F. X. Lee, S. J. Dong, T. Draper, I. Horvath, K. F. Liu, N. Mathur and J. B. Zhang, Nucl. Phys. Proc. Suppl. 119 (2003) 296; N. Mathur, F. X. Lee, A. Alexandru, C. Bennhold, Y. Chen, S.J. Dong, T. Draper, I. Horvath, K.F. Liu, S. Tamhankar and J. B. Zhang, Phys. Rev. D 70 (2004) 074508.
7. D. Galletly, M. Gürtler, R. Horsley, B. Joo, A. D. Kennedy, H. Perlt, B. J. Pendleton, P. E. L. Rakow, G. Schierholz, A. Schiller and T. Streuer, Nucl. Phys. Proc. Suppl. 129 (2004) 453.
8. W. Bietenholz, T. Chiarappa, K. Jansen, K. I. Nagai and S. Shcheredin, JHEP 0402 (2004) 023.
9. P. Hernandez, K. Jansen and M. Lüscher, Nucl. Phys. B552 (1999) 363.
10. G. Colangelo, Nucl. Phys. Proc. Suppl. 140 (2005) 120.
11. T. Bakeyev, D. Galletly, M. Göckeler, M. Gürtler, R. Horsley, B. Jo, A. D. Kennedy, B. Pendleton, H. Perlt, D. Pleiter, P. E. L. Rakow, G. Schierholz, A. Schiller, T. Streuer and H. Stüben, Nucl. Phys. Proc. Suppl. 128 (2004) 82.
12. M. Gürtler, R. Horsley, V. Linke, H. Perlt, P. E. L. Rakow, G. Schierholz, A. Schiller and T. Streuer, Nucl. Phys. Proc. Suppl. 140 (2005) 707.
13. L. Giusti, C. Hoelbling, M. Lüscher and H. Wittig, Comput. Phys. Commun. 153 (2003) 31.
14. M. Lüscher and P. Weisz, Commun. Math. Phys. 97 (1985) 59.
15. C. Gattringer, R. Hoffmann and S. Schaefer, Phys. Rev. D65 (2002) 094503.
16. K. Symanzik, Nucl. Phys. B226 (1983) 187.
17. M. Göckeler, R. Horsley, E.-M. Ilgenfritz, H. Perlt, P. Rakow, G. Schierholz and A. Schiller, Phys. Rev. D53 (1996) 2317.
18. G. Martinelli, C. Pittori, C. T. Sachrajda, M. Testa and A. Vladikas, Nucl. Phys. B445 (1995) 81.
19. J. A. Gracey, Nucl. Phys. B662 (2003) 247; Nucl. Phys. B667 (2003) 242.
20. R. Horsley, H. Perlt, P. E. L. Rakow, G. Schierholz and A. Schiller, Nucl. Phys. B693 (2004) 3 [Erratum-ibid. B **713** (2005) 601]; Phys. Lett. B628 (2005) 66.